Vol. 363: 171–182, 2008
doi: 10.3354/meps07463

MARINE ECOLOGY PROGRESS SERIES
Mar Ecol Prog Ser

Published July 15

3D visualization and quantification of marine benthic biogenic structures and particle transport utilizing computer-aided tomography

Rutger Rosenberg[1,*], Antoine Grémare[2], Jean Claude Duchêne[2], Earl Davey[3], Michael Frank[4]

[1]Department of Marine Ecology, Göteborg University, Kristineberg Marine Research Station, 45034 Fiskebäckskil, Sweden
[2]Université Bordeaux 1, UMR 5805 EPOC, Station Marine d'Arcachon, 2 Rue de Professeur Jolyet, 33120 Arcachon, France
[3]US Environmental Protection Agency, 27 Tarzwell Drive, Narragansett, Rhode Island 02882, USA
[4]Lysekil Hospital, Box 203, 45325 Lysekil, Sweden

ABSTRACT: Computer-aided tomography was used to visualize and quantify biogenic structures (e.g. burrows, shells) in 3 dimensions (3D) by scanning 9 replicate cores obtained from a 41 m deep station in the Gullmarsfjord (Skagerrak, western Sweden). The main objective was to visualize and quantify the biogenic structures and their volumes in the sediment. In addition, the particle transport was studied by adding an aluminum oxide tracer to the sediment–water interface (SWI), which was analysed after 57, 80 and 128 h, in 3 replicate cores each time. A new software programme was developed for rapid and accurate analysis. The fauna in the cores, analysed after scanning, were dominated by the brittle stars *Amphiura filiformis* and *A. chiajei*. The volumes of 'active' biogenic structures, defined as connecting to the SWI, were generally greatest close to the interface with some secondary peaks, probably related to the position of the disc chamber of the brittle stars. A mean volume of 560 cm^3 of biogenic structures per m^2 of sediment surface was recorded within the sediment (down to a mean depth of 137 mm, where the biogenic structures ceased to be 'active'). Ejection of particles to the SWI (mounding) was calculated to be between 4 and 40 $mm^3\ h^{-1}$.

KEY WORDS: Benthos · Bioturbation · Macrofauna · Tracer · Sediment · *Amphiura* spp.

INTRODUCTION

The marine ecosystem is difficult to comprehend as only minor parts can be visualized and studied at one time. In particular it is difficult to study animal behavioural and activity patterns *in situ*. Such constraints are indeed obvious for direct observations of sediment dwelling animals. Recordings of benthic animal behaviour have primarily been done under controlled conditions in aquaria, where a large variety of activity patterns of different species have been identified (Rhoads 1974), their functional roles described (Fauchald & Jumars 1979, Pearson 2001, Gerino et al. 2003) and generalized over depth (Pearson & Rosenberg 1987) and salinity gradients (Bonsdorff & Pearson 1999).

The impact of benthic animals on the physical properties and chemical conditions of sediments are manyfold and complex (Aller 1988, Dorgan et al. 2006). Burrowing, reworking and displacement of sediment particles by benthic fauna are generally referred to as bioturbation. Several models and mathematical approaches have been used to quantify the rate of particle transport (e.g. Francois et al. 2001, Gerino et al. 2003, Meysman et al. 2003). Particle transport is mainly studied and quantified within the sediment by applying different tracers (Gerino et al. 1994) and counting their appearance in sections of sliced sediment. New developments in optical and repeated image analysis have recently made 2-dimensional (2D) non-destructive quantification of particle reworking possible in experi-

*Email: rutger.rosenberg@marecol.gu.se

mental studies (Gilbert et al. 2003, Maire et al. 2006). However, biodeposition and bioresuspension, transports of significant ecological importance, have been poorly addressed in studies of particle transport (Davis 1993, Graf & Rosenberg 1997). The development of new techniques, such as video tracking in real time, has made it possible to follow the complexity of animal feeding behaviours such as rates and rhythms, and their impact on particles at the sediment–water interface (Duchêne & Rosenberg 2001, Grémare et al. 2004). Bioturbation and bioirrigation of benthic fauna are activities of great importance for various ecosystem-related functions such as redox conditions (Kristensen 2000) and nutrient fluxes (Furukawa et al. 2001, Mermillod-Blondin et al. 2004, Karlson et al. 2005a, Heilskov et al. 2006). In addition, mineralization rates in sediments are influenced by macrofaunal diversity (Emmerson et al. 2001, Mermillod-Blondin et al. 2005) as well as particular species traits (Norling et al. 2007).

Visualization in 2D of biogenic structures *in situ* has been possible by sediment profile imaging (SPI) since Rhoads & Cande (1971) invented this technique. SPI has been used for rapid assessment of benthic faunal successional stages and to relate such patterns to environmental benthic quality in general (Rhoads & Germano 1982, Rosenberg et al. 2004), to hypoxia (Nilsson & Rosenberg 1997) and for assessing the impact of fish farm activity (Karakassis et al. 2002). Radiographic techniques have proven useful for visualizing and quantifying benthic burrows (Charbonneau et al. 1997, Gerino et al. 1999). Recently, computer-aided tomography (CT), a diagnostic method used in hospitals, has been applied to visualize, in 3D, and quantify biogenic structures in marine sediment. The CT technique was initially used in the marine field in a pollution gradient study in Rhode Island, USA (Perez et al. 1999). Scientists in Canada later used this technique to estimate the space occupied by biogenic structures by depth in sediment from some different areas (Mermillod-Blondin et al. 2003, Michaud et al. 2003, Dufour et al. 2005). Recently a more detailed examination of the sediment from Swedish fjords was done using CT where, for example, the occupied space of recent and relic worm tubes and mollusk shells were visualized and quantified (Rosenberg et al. 2007). The present study benefits from the knowledge and development described in that recent publication.

The first aim of this study was to apply the CT technique to visualize and assess the space occupied by the benthic animals in a natural community dominated by the brittle star *Amphiura filiformis*. Second, CT analysis was also used to assess the faunal-mediated particle transport of an alumina tracer from the sediment–water interface down into the sediment. *A. filiformis* is a conspicuous species in many sublittoral areas in the northeast Atlantic Ocean (Duineveld et al. 1987) and may reach numbers of up to 3000 ind. m^{-2} (Rosenberg 1976, Josefson 1995). Vopel et al. (2003) estimated that a natural population of *A. filiformis* can account for 80% of the total flux of oxygen into the surface sediment. Crude estimates of the area occupied by this species within the sediment have been made in several studies (Ockelmann & Muus 1978, Rosenberg 1995, Solan & Kennedy 2002, O'Reilly et al. 2006), but this is the first time a detailed 3D visualization and examination of the biogenic structures of a community dominated by *A. filiformis* are presented.

MATERIALS AND METHODS

Core samples. On 21 April 2006, 9 samples were taken with an Olausson box corer (29 × 29 cm, 50 cm tall) at one 41 m deep station in the Gullmarsfjord on the Swedish Skagerrak coast (58° 14.67′ N, 11° 25.58′ E). From a 25 yr annual sampling record by the Swedish Monitoring Programme the benthic faunal composition at that station (Lyse 4) is known to have a long-term stability with a dominance of *Amphiura filiformis*, and the sediment to be sandy and silty clay with 50% of the particles >16 µm in size and a loss on ignition of 8.4% (Agrenius 2002). One PVC core tube (340 mm long and 153 mm internal diameter with a 5 mm wall thickness) was pushed into each sediment sample taken by the box corer for later CT scanning. Sediment surrounding the outside of the PVC core was removed and a core bottom and top was screwed into the coring tube. A few hours after sampling, the PVC cores were flushed with about 300 ml min^{-1} of running seawater of ambient salinity (33) at a constant temperature (8°C). The volume of water above the sediment was ~1 l.

On 22 April, 50 g of non-toxic alumina (aluminium oxide, Al_2O_3) was added to the surface of each core. The alumina was mixed with water in a jar, stirred and pored into a PVC cylinder with a 1 mm mesh screwed on top of each PVC core to get an even distribution of the particles (size, 40 µm; density, 3.3 g cm^{-3}). The alumina density was slightly higher than that of animal structures such as mollusk shells constructed from $CaCO_3$ (2.7 g cm^{-3}). The addition began at 08:30 h and was completed for all 9 cores within 1 h. The water flushing was interrupted during the addition of tracer, and restarted ~15 min later when the water above the sediment became transparent. The spread of the tracer appeared evenly on the surface and was ~1.5 mm thick. Shortly after the addition, considerable activity was seen on the surface: arms of brittle stars were in upright (filtering) position or searching the sediment surface.

The scanning times for the different cores after addition of the alumina were as follows: Cores 1, 2 and 3 after 57 h; Cores 4, 5 and 6 after 80 h; and Cores 7, 8 and 9 after 128 h. The sediment in the cores was stabilized for horizontal CT scanning, which, compared with vertical scanning, obtains the best CT image resolution (E. Davey, pers. obs.). This stabilization was done about 2 h before CT scanning; the PVC top was removed and the overlying water was carefully siphoned off the sediment. The sediment was then capped with a thick mixture of Cream of Rice® (Nabisco) and seawater until the space between the sediment–water interface (SWI) and the top of the core was filled. This technique is superior to that used by Rosenberg et al. (2007). Tops of the PVC cores were reattached before CT scanning to ensure the sediment remained as intact as possible.

Every sediment core was sieved on a 1 mm screen the morning after it had been scanned. All organisms appeared to be alive after sieving. The organisms were removed from the sieve, identified to species or taxa, counted and photographed together with other objects such as empty shells and tubes to assist in the groundproofing of the CT analyses. The diameters of the discs of 10 randomly chosen individuals of *Amphiura filiformis* were between 4 and 7 mm (mean 5.8 mm) and the lengths of the arms were between 35 and 93 mm (mean 63 mm).

CT scanning. All cores were CT scanned at the Lysekil Hospital, Sweden, using a Siemens model Sensation 4 medical scanner, at a slice thickness of 1.0 mm, power settings of 120 kV and 175 mA, and a pitch of 1. The sediment cores were oriented in a horizontal position (rotated 90° from the vertical as collected in the field, lying down for between 90 and 120 s and scanned along the axis of uniform circular cross-sections). All image data for each sediment core were stored in a universal medical format called DICOM. When a 2D CT image is generated, it is composed of pixels (a single area of equal length and width) that are each associated with a specific CT number. When a 3D image is generated, it is composed of voxels (representing units of volume), which are pixels with a depth defined by the selected slice thickness. In this investigation, the image pixel size was 0.37 × 0.37 mm and the slice thickness 1.0 mm, which means each voxel was equal to 0.1369 mm^3.

The original sediment CT procedures are described by Perez et al. (1999) and summarized online (www.epa.gov/aed/html/ct/index.html). Recently the original method was developed further to include analyses of space occupied by recent and relic worm tubes, and of live shells in the sediment as well as quantification of volumes occupied by biogenic structures (Rosenberg et al. 2007). In that study, calibration rods having different densities were pushed vertically into the sediment before scanning as a reference to CT numbers of different objects' densities. The following CT ranges, which are related to the medical Houndsfield Unit ranges by adding –1000 to the CT ranges, were used in the analysis: gas 0–900, water 901–1250, sediment 1251–1800, and shells 1801–4000. Alumina should be in the same CT range as that for shells. These calibrated ranges should be particularly relevant as the same scanner was used in the present study. Thus, these CT ranges were used in this study to compute the presence of different biogenic structures and other objects in relation to the presence of gas, water, sediment and shells based on the digital information in each section of each core. Detailed information about CT procedures used in this study is given in Rosenberg et al. (2007).

CT image analysis. The CT digital information of each core was analysed to obtain the volume of water in tubes and burrows connected to the SWI. Water found at some depth in the sediment and not connected to the SWI was considered to be mainly water in relic worm tubes (Rosenberg et al. 2007). The volume of alumina tracer and shells was computed when they occurred below the SWI and were present within animal burrows (see details in following paragraphs). From the images it was obvious that several thin burrows (probably of arms of *Amphiura filiformis* and *A. chiajei* connecting to the SWI) collapsed close to the SWI while scanning the cores in a horizontal position. Such structures were included in the analysis if the distance to the SWI was less than 10 voxels (i.e. 10 mm).

A software programme (developed by J. C. Duchêne) was used for the CT image analysis as follows. Computation of the SWI provided a 3D interface of the sediment, saved as a grey-level image, and reconstructed as a 3D mesh file. This involved 2 main steps. First, the supernatant water was labelled, which eliminated all rice powder particles providing signals in the sediment channel and sediment particles that were above and not connected to the sediment surface. This labelling process designated water voxels, as the floodfill procedure propagated inside the funnels and tubes connected to the supernatant water. Second, the SWI was demarcated, which could be composed of sediment or alumina particles settled upon the surface to form a layer that had not yet been bioturbated. Sediment may be interface sediment or sediment transported by animal activity. The different computations are presented in Table 1 and Fig. 1 and described in the following paragraphs. Origin of the graphs may use 2 different interfaces: (1) the upper side of aluminate surface layer, i.e. between the lower part of Label 5 and the upper part of Label 6; (2) the SWI, i.e. between the lower part of Label 6 and the upper part of Label 3.

Table 1. Labels used to discriminate numeric objects in the sediment cores for the assessment of biogenic structures and alumina including definitions of 'biogenic aluminate' and 'biogenic water'. Examples of the numeric object are visualized in Fig. 1

Label	Description
1	Gas bubbles in the sediment
2	Water voxels (not included in other labels)
3	Sediment voxels
4	Aluminate/carbonate voxels (not included in other labels)
5	Supernatant water (between surface and first non-water voxels)
6	Aluminate surface layer (remainder of initial aluminate layer)
7	Mounded sediment layer (sediment ejected over the initial aluminate layer by action of benthic organism)
8	Surface-connected water
9	Aluminate connected to the surface through Label 8
10	Water connected to the surface through Labels 8 and 9
11	Surface-connected aluminate
12	Water connected to the surface through Label 11
13	Water patches not connected to the surface and not adjacent to aluminate with volume > threshold[a]
14	Aluminate/carbonate patches not connected to the surface with volume > threshold[a]
15	Aluminate small patches inside sediment (Label 4) adjacent by at least 1 voxel to water voxels (Label 2)
16	Water small patches inside sediment (Label 2) adjacent by at least 1 voxel to aluminate/carbonate voxels (Label 4)
18	Water within depth[b] area not connected to the surface with volume > threshold[a] and adjacent to aluminate
20	Aluminate within depth[b] area not connected to the surface with volume > threshold[a] and adjacent to water (i.e. collapsing and *Amphiura* chambers)

[a]Threshold: 20 mm^3 (150 voxels)
[b]Depth: area between sediment interface and lower depth of any voxel of biogenic structures (Labels 8 to 12)
Biogenic tracer = Label 9 + Label 11 + Label 20
Biogenic water = Label 8 + Label 10 + Label 12 + Label 18

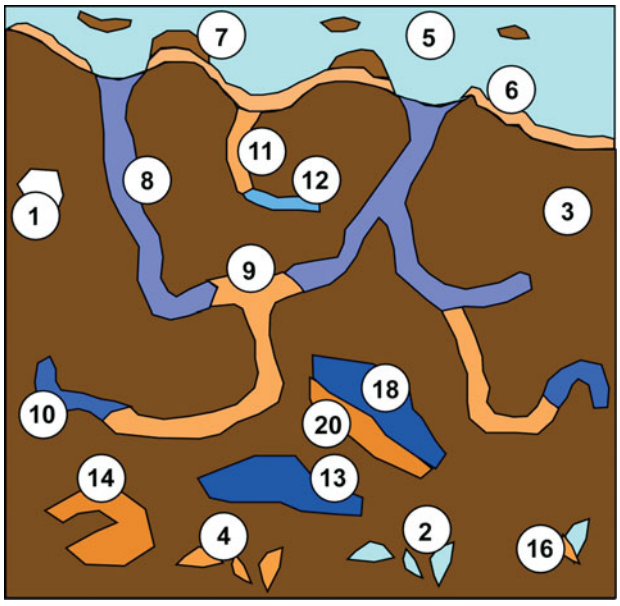

Fig. 1. Different objects analysed in the sediment, computed as described in Table 1

By comparing the surface covered by alumina and the sediment surface, apertures of tubes and funnels were isolated and closed after a 3D smoothing process. This allowed computation of (1) the supernatant volume (Label 5; Table 1), (2) the volume of sediment ejected on the sediment surface (mounding) by animal activity above the alumina tracer (Label 7), (3) the volume of water voxels in tubes directly connected to the surface water (Label 8), and (4) the volume of the remaining alumina cover (Label 6).

Some tubes (Label 9) were filled with alumina and connected to the surface through portions of tubes filled with water (Label 8). The 3D floodfill procedure extended the labelling inside the sediment and also along the tube walls where bioturbated alumina was deposited against the walls. Captive water inside tubes was computed as water pockets isolated from the surface by alumina gaps (Label 10).

Tube structures filled by the initial alumina layer (Label 11) and captive water isolated from the surface by these structures (Label 12) were searched for and analysed. Isolated blobs of water voxels (Label 13) and alumina voxels (Label 14) were analysed when present. Volumes under 20 mm^3 were not accounted for inside the sediment (a threshold [see Table 1] of 150 voxels corresponded to water or alumina blobs with a diameter < 3.4 mm). The smallest blobs were found throughout the sediment and may correspond to older collapsing events. The larger patches were separated from the surface due to collapse of the tubes, which probably occurred during the transport of the cores and/or scanning the cores in a horizontal position. The alumina connected to the inside of these pockets was labelled (Label 15) when depth of the upper voxel in the patch was located between the sediment interface and depth of the lowest voxel of all the biogenic tubes (Labels 8 to 12). The programme isolates small gas volumes (Label 1), small water vol-

umes (Label 2) and small alumina or shell fragment volumes (Labels 4 and 16). This results in a 3D label matrix that presents these diverse components.

The next step was computation of the vertical profiles for every point of the sediment surface. These profiles were shifted upward to have a zero line starting at the initial SWI and summed. Filters were applied to eliminate blobs that were located below a limit provided to the program as the lower limit of activity. Various filters allowed the elimination of water, alumina or shell fragment volumes deep inside the sediment, depending on their shape (using volume:surface ratio, greater length obtained by 3D thinning algorithm, position of bounding boxes).

The 'biogenic water,' i.e. water in biogenic structures and generally connected to the SWI, was a summation of Labels 8, 10, 12 and 18. The 'biogenic tracer,' i.e. aluminate transported by the animals, was a summation of Labels 9, 11 and 20 (Table 1).

Differences between volumes in cores were tested by ANOVA. Correlations between volumes of biogenic water and tracer were analysed by linear correlation.

RESULTS

Fauna collected in cores

The benthic fauna in the cores were numerically dominated by the brittle star *Amphiura filiformis*, generally found in numbers of between 20 and 37 per core, except in Core 1 where only 11 individuals were present (Table 2). This was equal to an approximate density of between 610 and 2055 per m^2. Second in dominance was *A. chiajei*, followed by the polychaetes *Nephtys incisa* and *Diplocirrus glaucus*.

Table 2. Taxa and their abundance found in each core after scanning

Taxon	Core no.								
	1	2	3	4	5	6	7	8	9
Amphiura filiformis	11	34	27	20	27	27	28	37	23
Amphiura chiajei	3	2	3	2	6	3			7
Nephtys incisa	1	1	1	1		1	1		
Eteone longa	1								
Polyphysia crassa	1				1			2	2
Diplocirrus glaucus			1	1	1	1		3	1
Pectinaria belgica						1			
Glycera rouxii									
Golfingia sp.			1					1	
Thyasira sp.	1								
Myrtea spinifera						1			
Nucula sp.				1	1				
Cerebratulus sp.								1	
Turbellaria					1				
Pennatula phosphorea						2			

Biogenic structures and particle displacement

When the CT range for water in Cores 4 and 6 was visualized in 3D, the general appearance in the sediment was as follows. There were a vast number of water filled, predominantly vertical to diagonal, elongated biogenic structures mainly down to about 6 to 7 cm below the SWI (Fig. 2A,B). The structures were generally thin close to the SWI, and somewhat wider farther down in the sediment. Most of these thin structures were interpreted to be burrows of the arms of *Ampiura filiformis* and *A. chiajei* connecting to the discs at several centimeters depth in the sediment. Some large, cylindrical structures in Fig. 2C may be burrows of *Nephtys incisa*. 3D visualizations of biogenic structures with water and tracers combined are shown in Fig. 2C (Core 6) and Fig. 2D (Core 5). This shows that the tracer below the SWI was located in burrows and sometimes concentrated at their deepest and enlarged extensions (Fig. 2D). Some of these voids may be disc chambers of *Amphiura chiajei* or *A. filiformis*, as these 2 species occurred in high numbers in this core. Distribution of the aluminum tracer in Core 6 is visualized separately in Fig. 2E. Most of the tracer was found close to the SWI, but some of it had been transported down in the burrows. Finally, in Fig. 2F objects that were not by definition connected to the SWI were also included. Most of these structures were probably shell fragments (as they appeared in that same CT range), but some could be alumina tracers in collapsed burrows not connected to the SWI. Thus, the particle transport could be underestimated. Some water filled structures deeper down in this image were probably relic tubes and burrows.

The number of voxels was parameterized in each core to calculate (1) the volume of biogenic water, (2) volume biogenic alumina, and (3) volume of these 2 variables combined, which equals the volume of biogenic structures. These calculations are presented as volumes within the sediment per mm^2 of sediment surface area (Fig. 3). The biogenic structures with connections to the SWI had a vertical distribution down to a mean of 13.7 cm in the sediment. The volume of water in the burrows in each core was always greater than the volume of tracer. Mean volumes of biogenic water, biogenic tracer and biogenic structure were 0.47, 0.08 and 0.56 $mm^3\ mm^{-2}$, respectively. The total volume of biogenic structures varied between 0.39 and 0.94 $mm^3\ mm^{-2}$. There was no temporal trend over the scanning period; the volume of tracer in the burrows was lowest at the first scanning, but did not increase after the second scanning.

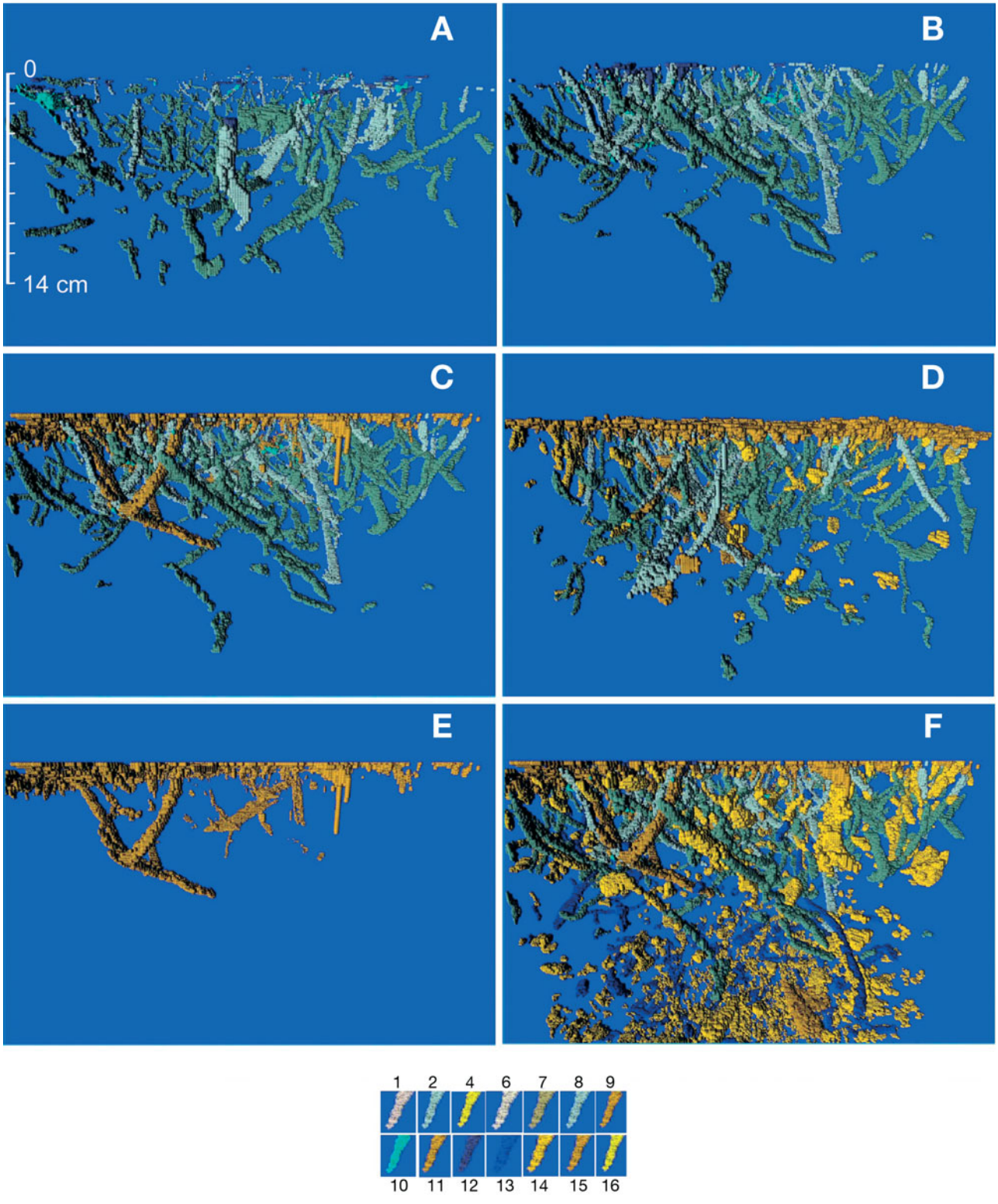

Fig. 2. 3D visualization of structures with water and/or tracer in animal burrows in the sediment. (A & B) Water in Cores 4 and 6, respectively (CT range 901–1250); (C & D) water (green) and tracer (yellow) (CT range 1801–4000) combined in Cores 6 and 5, respectively; (E) tracer in Core 6; (F) water (CT range 901–1250), tracer, shells and shell debris (CT range 1801–4000) in Core 6. Code to the different colours is provided at the bottom of the figure with numbers corresponding to labels described in Table 1 and Fig. 1

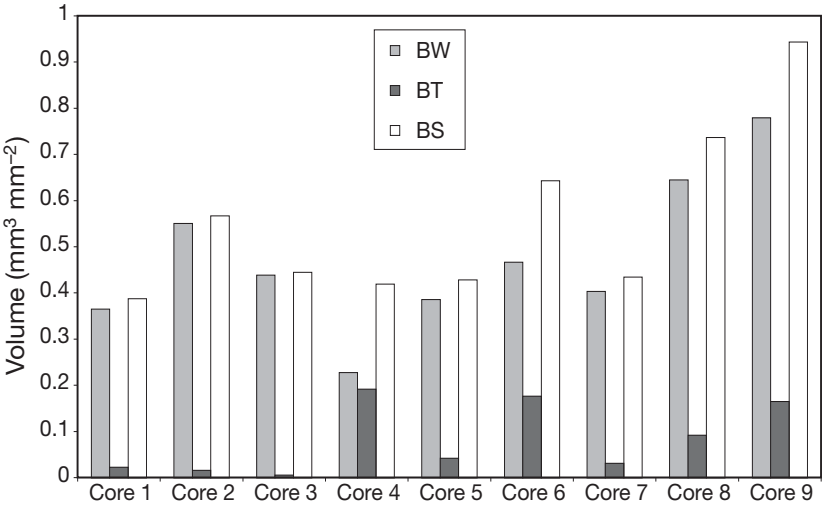

Fig. 3. Volumes of biogenic water (BW), biogenic tracer (BT) and water and tracer combined (biogenic structure, BS) within the sediment in $mm^3\ mm^{-2}$ of sediment surface area in the different cores

Vertical distribution of the calculated volumes of biogenic water and biogenic tracer in the 9 cores is shown in Fig. 4. The vertical profiles of biogenic water had 2 peaks in several cores (particularly Cores 1, 2, 3, 8 and 9), the first peak between 20 to 30 mm and the second around 60 mm depth in the sediment. No biogenic structures with connections to the SWI were found deeper than 170 mm.

The mean amount of sediment ejected per hour on the sediment surface above the alumina tracer was computed in the 9 cores (Fig. 5). Overall, a high activity was recorded at the first scanning after 57 h, and it was generally lowest in the cores scanned after 80 h. This mounding was calculated to between about 4 and 40 $mm^3\ h^{-1}$.

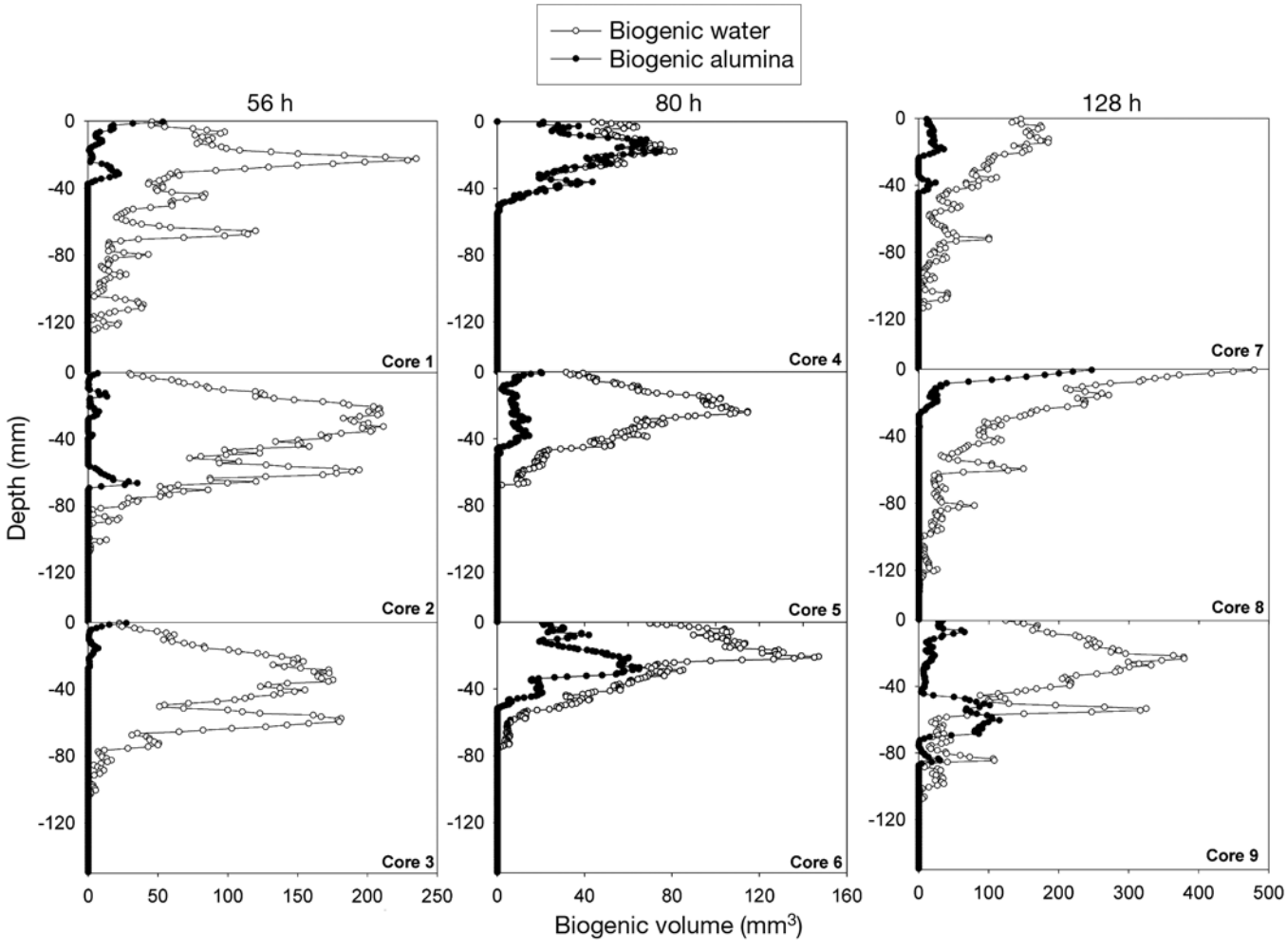

Fig. 4. Volumes (mm^3) of (○) biogenic water and (●) biogenic tracer (alumina) in the different cores versus depth (mm). Cores 1 to 3 scanned after 56 h, Cores 4 to 6 after 80 h and Cores 7 to 9 after 128 h

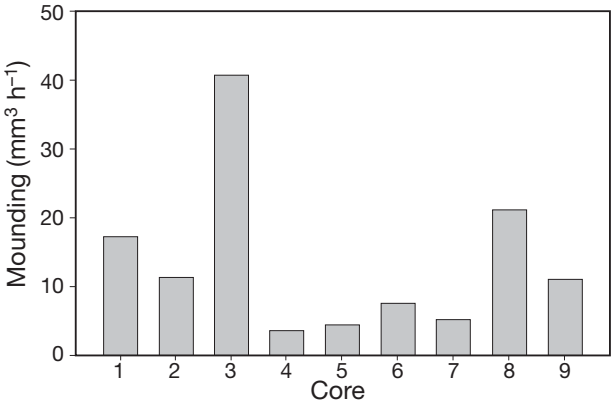

Fig. 5. Mounds produced at the sediment–water interface per hour, probably most often by *Amphiura filiformis*, in Cores 1 to 9 calculated from the computation described as Label 7 in Table 1. Cores 1 to 3 scanned after 56 h, Cores 4 to 6 after 80 h and Cores 7 to 9 after 128 h

DISCUSSION

Quality of methods used

All animals were alive after CT scanning, which demonstrated that rice-capping the sediment surface and putting the cores in horizontal position for the best scanning resolution for ~2 min did not have any serious effects on their condition. The addition of the alumina tracer had no visual effect on the activity of *Amphiura filiformis* as their arms were active in a similar way as prior to introducing the tracer. Thus, these observations suggest that the 3D visualization and the assessment of the volumes of the biogenic structures could produce an accurate reproduction of natural conditions.

The quantification of the alumina tracer in the sediment was mainly restricted to its appearance in burrows that were connected to or very close to the SWI. By this procedure, the occurrence of the tracer was separated from shells and shell debris mainly occurring deep down in the cores (Fig. 2F). The particle size (40 µm) of the tracer was within the range of the natural sediment, where half of the particles were >16 µm. Earlier experiments have shown that *Amphiura filiformis* has an immediate and strong response to addition of phytodetritus to the sediment surface (Duchêne & Rosenberg 2001). In the present study, many of the arms of *A. filiformis* stretched into the water column as in a filtering position. Thus, the active transport of tracer into the sediment was considered to be lower compared with that for added phytodetritus and will most likely result in a more conservative assessment of particle transport than when compared with particles that may contain organic material.

Visualization and assessment of structures of *Amphiura*

In the present study, the impressive network of arms of *Amphiura filiformis* particularly, and to a lesser extent of *A. chiajei*, was visualized in 3D for the first time. The structures were mainly orientated vertically from the SWI and down to a depth of about 6 to 7 cm, where the discs were probably located. The vertical profiles of biogenic water showed a bimodal pattern in 5 of 9 cores, where the upper peak could be related to activity of the arms of the brittle stars and the lower peak at ~60 mm to the position of the disc. *Amphiura filiformis* has a wide distribution in the North Sea (Duineveld & van Noort 1986, Künitzer et al. 1992) and in the Skagerrak–Kattegat (Josefson 1995, Rosenberg 1995). The number of burrow structures would be even greater in nature than estimated in this study, as some burrows may have collapsed and been disconnected from the SWI during the capping and horizontal scanning of the cores. The large number of *Amphiura* burrows connecting to the SWI support earlier conclusions that the species has a significant impact on the supply of oxygen into the sediment (Vopel et al. 2003). Moreover, *A. filiformis* has a significant density-dependent effect on the oxygen consumption and on nutrient fluxes out of the sediment (Karlson et al. 2005b). Even if individuals of *A. filiformis* remained in the same position for some time and reinforce their burrows with mucus (Woodley 1975), their activity pattern could be stimulated or distressed by external factors such as light regime (Rosenberg & Lundberg 2004), tidal regime (Solan & Kennedy 2002), oxygen concentrations (Rosenberg et al. 1997), food availability (Duchêne & Rosenberg 2001), predators (Rosenberg & Selander 2000), and by density-dependent intraspecific competition (Rosenberg et al. 1997). These activity patterns of *A. filiformis* involve movements of discs and arms, which will displace the sediment and produce changes of sediment redox conditions and solute fluxes. As many burrows were visualized to connect to the SWI, the mucus lining probably kept most of them intact when actively used by the brittle stars.

CT and other techniques for analysing biogenic structures

Since the pioneering work by Perez et al. (1999), the use of CT for analyzing biogenic structures in marine sediments have been used in several Canadian studies (Mermillod-Blondin et al. 2003, Michaud et al. 2003, Dufour et al. 2005). In these studies (op. cit.) the space occupied by biogenic structures were analysed by using a fixed tomographic intensity (TI) value, and all

pixels associated with higher TI values were classified as sediment and all lower values as biogenic structures. Thus, this simplified analysis did not separate structures connected to the sediment surface from those that were not connected, and the analytical technique did not include the biovolume of animals living within shells or dense worm tubes. Although the method was improved in the latter study to obtain a better and quicker analysis, it is not clear how accurate the assessments were because most of the water within the cores had leaked out before scanning (Dufour et al. 2005). Another technique used to analyse biogenic structures in sediment was to slice sediment in thin sections and to digitally analyse each section for structures such as burrows, tubes and shells (Rosenberg & Ringdahl 2005).

Solan & Kennedy (2002) measured the volume and displacement of the disc cavity of *Amphiura filiformis* in sediment profile images in Galway Bay, Ireland. The volume was calculated from the visible burrow void against the camera faceplate assuming that this was half a cylinder. Similarly, O'Reilly et al. (2006) showed from the same study area and using a similar technique that the disc chamber area changed over time. The advantage with this technique was that the void was visualized and that volumes could be estimated. In comparison, the CT technique will measure both the voids and the burrows in 3D with high accuracy, as both water and the calcified body were included in the analysis.

Estimates of volumes of biogenic structures in the sediment at another station in the Gullmarsfjord at 75 m, with comparatively lower numbers of *Amphiura filiformis* (120 to 183 ind. m^{-2}), gave much lower values: 4.2 to 8.0 cm^3 m^{-2} of sediment surface area (Rosenberg & Ringdahl 2005), compared with a mean of about 560 cm^3 m^{-2} (range 390 to 940 cm^3 m^{-2}) in the present study. This difference could be a result of much higher numbers of brittle stars in the present study or better methods for quantification of volumes. The corresponding biogenic area to that volume was not calculated in this study.

Ockelmann & Muus (1978) calculated that 1 adult brittle star could occupy an area of 35 cm^2. Based on that value, Rosenberg (1995) calculated that a dense *Amphiura filiformis* population (3000 ind. m^2) in the Skagerrak could increase the area within the sediment by 10 times compared with that of the surface. Solan & Kennedy (2002) calculated that 1 individual of *A. filiformis* in Galway Bay increased the surface area in the sediment by ~20 cm^2. With a density of 700 ind. m^{-2} in that bay, the area enlargement within the sediment was calculated as 1.4 m^2 m^{-2}. Other scientists (summarized by Welsh 2003) have estimated that burrows may increase the area within the sediment by 1.5 to 5 times compared with that of the surface. Rosenberg & Ringdahl (2005) used a method to digitize vertical slices of sediment at a station in the Gullmarsfjord with *A. filiformis* present, and found that the subsurface area with biogenic structures was 1.4 to 1.7 m^2 m^{-2}. The volumes of biogenic structures in the present study were lowest in Core 1, which had the lowest number of individuals of all cores. Abundance and/or particular species traits could be important for how large the subsurface biogenic structures are. In summary, the areas occupied by burrow structures in the sediment are of significant ecological importance. Their quantification is dependent upon accurate assessment of the burrow sizes and their numbers.

Methods other than CT have been used to visualize burrow and tunnel systems in sediments. For example, resin casts have been used to demonstrate the architecture of impressive tunnel structures made by thallassinidean crustaceans (Astall et al. 1997) and complex networks of burrows made by polychaetes (Davey 1994). However, that technique has its limitations because it can only be used in laboratory studies or in shallow waters, and minor structures, such as arm burrows of *Amphiura filiformis*, cannot be quantified.

In summary, CT is a technique that can visualize biogenic structures in the sediment and the analysis of the image data can be used to calculate the volumes of various structures such as burrows and shells separately. The technique has also proven accurate for sediment grain size assessment and for separating live and relic worm tubes (Rosenberg et al. 2007). At present, no other methods exist that have such scientific advantages. However, the CT method could be improved by further development of software that could yield a quicker analysis. Also, scanning of sediment in a vertical position would have advantages, e.g. scanning the same core over multiple time periods. However, since the resolution of sediment images in present day standard medical CT instruments designed for humans is better for vertical compared with horizontal scanning, other CTs such as medical research micro-CT or industrial CT machines might be better for this purpose.

Particle transport

Josefson et al. (2002) studied the vertical activity in a community dominated by *Amphiura filiformis* in the inner part of the Gullmarsfjord, i.e. the same fjord as in the present study. They found a strong activity in the upper 6 cm of the sediment based on ^{14}C profiles. O'Reilly et al. (2006) used tracers to observe and calculate vertical profiles of their distribution in the sediment against the faceplate of a sediment profile camera. They showed that *A. filiformis* can create mounds

on the sediment surface, and that transport of sediment will eventually cover tracers put on the sediment surface. O'Reilly et al. (2006) estimated that the mounding at the SWI calculated at the faceplate of a sediment profile camera could be around 20 mm^2. In the present study, the mounding was calculated as 2 to 40 $mm^3\ h^{-1}$. As mounding has mainly been described in *A. filiformis* before, we assume that most of the ejection was due to the activity of this brittle star. Thus, transport from the sediment to the SWI could be a process of ecological significance, but it also seems highly variable. Based on the 3D visualization of the aluminum tracer in the present study, it was obvious that displacement from the SWI down to depths of several centimeters occurred within days. The volume of tracer in the sediment was lowest at the first scanning, but no further increase was recorded from the second to the third scanning. Thus, the main particle transport occurred within 80 h after the tracer was introduced. There is strong indication that the brittle stars were actively involved in this transport. Duchêne & Rosenberg (2001) showed that *A. filiformis* promptly reacts to phytodetritus added to the sediment surface and begins subducting such material within minutes.

Many studies have assessed the transport by bioturbation of macrobenthic invertebrates by models of biodiffusivity (D_b) (e.g. Gerino et al. 1994). In most of these studies various tracers have been used and their vertical transport measured by slicing the sediment in sections and quantifying the temporal transport of the tracer. Thus, the transport has generally been measured from start to end of an experiment without any temporal resolution and detailed information within each slice. Gilbert et al. (2003) used the optode technique to optically analyse, in 2D, changes in particle distribution related to the activity of *Amphiura filiformis*. Maire et al. (2006) took time series photographs of the sides of thin aquaria treated with fluorescent particles and assessed the temporal change in D_b. In the present study, the CT technique was used for the first time to visualize the distribution of a tracer in 3D. A large part of the particle transport is clearly nonlocal rather than diffusive transport, which has been found in several studies (Maire et al. 2007). The use of diffusive transport calculations in such cases will inadequately represent the particle transport rates.

LITERATURE CITED

Agrenius S (2002) Övervakning av mjukbottenfaunan längs Sveriges västkust. Rapport från verksamheten 2001, Marin Ekologi, Göteborgs Universitet

Aller RC (1988) Benthic fauna and biogeochemical processes in marine sediments: the role of burrow structures. In: Blackburn TH, Sørensen J (eds) Nitrogen cycling in coastal marine environments. John Wiley & Sons, Chichester, p 301–338

Astall CM, Taylor AC, Atkinson RJA (1997) Behavioural and physiological implications of a burrow-dwelling lifecycle for two species of upogebiid mud-shrimp (Crustacea: Thalassinidea). Estuar Coast Shelf Sci 44:155–168

Bonsdorff E, Pearson TH (1999) Variation in the sublittoral macrozoobenthos of the Baltic Sea along environmental gradients: a functional-group approach. Aust J Ecol 24: 312–326

Charbonneau P, Hare L, Carignan R (1997) Use of X-ray images and contrasting agent to study the behavior of animals in soft sediments. Limnol Oceanogr 42:1823–1828

Davey JT (1994) The architecture of burrow of *Nereis diversicolor* and its quantification in relation to sediment–water exchange. J Exp Mar Biol Ecol 179:115–129

Davis WR (1993) The role of bioturbation in sediment resuspension and its interaction with physical shearing. J Exp Mar Biol Ecol 171:187–200

Dorgan KM, Jumars PA, Johnson BD, Boudreau BP (2006) Macrofaunal burrowing: the medium is the message. Oceanogr Mar Biol Ann Rev 44:85–121

Duchêne JC, Rosenberg R (2001) Marine benthic faunal activity patterns on a sediment surface assessed by video numerical tracking. Mar Ecol Prog Ser 223:113–119

Dufour SC, Desrosiers G, Long B, Lajeunesse P and others (2005) A new method for three-dimensional visualization and quantification of biogenic structures in aquatic sediments using axial tomodensitometry. Limnol Oceanogr Methods 3:372–380

Duineveld GCA, van Noort GJ (1986) Observations on the population dynamics of *Amphiura filiformis* (Ophiuroidea: Echinodermata) in the Southern North Sea and its exploitation by the dab, *Limanda limanda*. Neth J Sea Res 20:85–94

Duineveld GCA, Künitzer A, Heyman RP (1987) *Amphiura filiformis* (Ophiuroidea: Echinodermata) in the North Sea. Distribution, present and former abundance and size composition. Neth J Sea Res 21:317–329

Emmerson MC, Solan M, Emes C, Paterson D, Raffaelli DG (2001) Consistent patterns and idiosyncratic effects of biodiversity in marine ecosystems. Nature 411:73–77

Fauchald K, Jumars P (1979) The diet of worms: a study of polychaete feeding guilds. Oceanogr Mar Biol Ann Rev 17:193–284

Francois F, Poggiale JC, Durbec JP, Stora G (2001) A new model of bioturbation for functional approach to sediment reworking resulting from macrobenthic communities. In: Aller JY, Woodin SA, Aller RC (eds) Organism–sediment interactions, Vol 21. University of South Carolina Press, Columbia, SC, p 73–86

Furukawa Y, Bentley SJ, Lavoie DL (2001) Bioirrigation modeling in experimental benthic mesocosms. J Mar Res 59: 417–452

Gerino M, Stora G, Durbec JP (1994) Quantitative estimation of biodiffusive and bioadvective sediment mixing: *in situ* experimental approach. Oceanol Acta 17:547–554

Gerino M, Stora G, Weber O (1999) Evidence of bioturbation in the Cap-Ferret Canyon in the deep northeastern Atlantic. Deep-Sea Res II 46:2289–2307

Gerino M, Stora G, François-Carcaillet F, Gilbert F and others (2003) Macro-invertebrate functional groups in freshwater and marine sediments: a common mechanistic classification. Vie Milieu 53:221–231

Gilbert F, Hulth S, Strömberg N, Ringdahl K, Poggiale JC (2003) 2-D optical quantification of particle reworking activities in marine sediments. J Exp Mar Biol Ecol

285-286:251–263
Graf G, Rosenberg R (1997) Bioresuspension and biodeposition: a review. J Mar Syst 11:269–278
Grémare A, Duchêne JC, Rosenberg R, David E, Desmalades M (2004) Feeding behaviour and functional response of *Abra ovata* and *A. nitida* compared by image analysis. Mar Ecol Prog Ser 267:195–208
Heilskov AC, Alperin M, Holmer M (2006) Benthic fauna bioirrigation effects on nutrient regeneration in fish farm sediments. J Exp Mar Biol Ecol 339:204–225
Josefson AB (1995) Large-scale estimate of somatic growth in *Amphiura filiformis* (Echinodermata: Ophiuroidea). Mar Biol 124:435–442
Josefson AB, Forbes TL, Rosenberg R (2002) Fate of phytodetritus in marine sediments: functional importance of macrofaunal community. Mar Ecol Prog Ser 230:71–85
Karakassis I, Tsapakis M, Smith CJ, Rumohr H (2002) Fish farming impacts in the Mediterranean studied through sediment profiling imagery. Mar Ecol Prog Ser 227: 125–133
Karlson K, Hulth S, Ringdahl K, Rosenberg R (2005a) Experimental recolonisation of Baltic Sea reduced sediments: survival of benthic macrofauna and effects of nutrient cycling. Mar Ecol Prog Ser 294:35–49
Karlson K, Ringdahl K, Hulth S, Rosenberg R (2005b) Density of bioturbating macrofauna and sediment biogeochemistry: *Amphiura filiformis* as model species. In: Karlson K (author) Impact of benthic macrofauna on sediment biogeochemistry—the importance of bottom water oxygen concentrations. PhD thesis, Göteborg University
Kristensen E (2000) Organic matter diagenesis at the oxic/anoxic interface in coastal marine sediments, with emphasis on the role of burrowing animals. Hydrobiologia 426: 1–24
Künitzer A, Basford D, Craeymeersch JA, Dewarumez JM and others (1992) The benthic infauna of the North Sea: species distribution and assemblages. ICES J Mar Sci 49: 127–143
Maire O, Duchêne JC, Rosenberg R, de Mendonca JB Jr, Grémare A (2006) Effects of food availability on sediment reworking in *Abra ovata* and *A. nitida.* Mar Ecol Prog Ser 319:135–153
Maire O, Duchêne JC, Grémare A, Malyuga VS, Meysman FJR (2007) A comparison of sediment reworking rates by the surface deposit-feeding bivalve *Abra ovata* during summertime and wintertime, with a comparison between two models of sediment reworking. J Exp Mar Biol Ecol 343:21–36
Mermillod-Blondin F, Marie S, Desrosiers G, Long B, de Montety L, Michaud E, Stora G (2003) Assessment of the spatial variability of intertidal benthic communities by axial tomodensitometry: importance of fine-scale heterogeneity. J Exp Mar Biol Ecol 287:193–208
Mermillod-Blondin F, Rosenberg R, François-Carcaillet F, Norling K, Mauclaire L (2004) Influence of bioturbation by three benthic infaunal species on microbial communities and biogeochemical processes in marine sediment. Aquat Microb Ecol 36:271–284
Mermillod-Blondin F, François-Carcaillet F, Rosenberg R (2005) Biodiversity of benthic invertebrates and organic matter processing in shallow marine sediments: an experimental study. J Exp Mar Biol Ecol 315:187–209
Meysman FJR, Boudreau BP, Middelburg JJ (2003) Relations between local, nonlocal, discrete and continuous models of bioturbation. J Mar Res 61:391–410
Michaud E, Desrosiers G, Long B, de Montety L and others (2003) Use of axial tomography to follow temporal changes of benthic communities in an unstable sedimentary environment (Baie des Ha! Ha!, Saguenay Fjord). J Exp Mar Biol Ecol 285–286:265–282
Nilsson HC, Rosenberg R (1997) Benthic habitat quality assessment of an oxygen stressed fjord by surface and sediment profile images. J Mar Syst 11:249–264
Norling K, Rosenberg R, Hulth S, Grémare A, Bonsdorff E (2007) Importance of functional biodiversity and species-specific traits of benthic fauna for ecosystem functions in marine sediment. Mar Ecol Prog Ser 332:11–23
O'Reilly R, Kennedy R, Patterson A (2006) Destruction of conspecific bioturbation structures by *Amphiura filiformis* (Ophiuroidea): evidence from luminophore tracers and *in situ* time-lapse sediment-profile imagery. Mar Ecol Prog Ser 315:99–111
Ockelmann KW, Muus K (1978) The biology, ecology and behaviour of the bivalve, *Mysella bidentata.* Ophelia 17: 1–93
Pearson TH (2001) Functional group ecology in soft-sediment marine benthos: the role of bioturbation. Oceanogr Mar Biol Ann Rev 39:233–267
Pearson TH, Rosenberg R (1987) Feast and famine: structuring factors in marine benthic communities. In: Gee JHR, Giller PS (eds) 27th Symposium of the British Ecological Society, Aberystwyth 1986. Blackwell Scientific Publications, Oxford, p 373–395
Perez KT, Davey EW, Moore RH, Burn PR and others (1999) Application of computer-aided tomography (CT) to the study of estuarine benthic communities. Ecol Appl 9: 1050–1058
Rhoads DC (1974) Organism–sediment relations on the muddy sea floor. Oceanogr Mar Biol Ann Rev 12:263–300
Rhoads DC, Cande S (1971) Sediment profile camera for *in situ* study of organism–sediment relations. Limnol Oceanogr 16: 110–114
Rhoads DC, Germano JD (1982) Characterization of organism–sediment relations using sediment profile imaging: an efficient method of remote ecological monitoring of the seafloor (Remots™ System). Mar Ecol Prog Ser 8:115–128
Rosenberg R (1976) Benthic faunal dynamics during succession following pollution abatement in a Swedish estuary. Oikos 27:414–427
Rosenberg R (1995) Benthic marine fauna structured by hydrodynamic processes and food availability. Neth J Sea Res 34:303–317
Rosenberg R, Lundberg L (2004) Photoperiodic activity pattern in the brittle star *Amphiura filiformis.* Mar Biol 145: 651–656
Rosenberg R, Ringdahl K (2005) Quantification of biogenic 3-D structures in marine sediments. J Exp Mar Biol Ecol 326:67–76
Rosenberg R, Selander E (2000) Alarm signal response in the brittle star *Amphiura filiformis.* Mar Biol 136:43–48
Rosenberg R, Nilsson HC, Hollertz K, Hellman B (1997) Density-dependent migration in an *Amphiura filiformis* (Amphiuridae, Echinodermata) infaunal population. Mar Ecol Prog Ser 159:121–131
Rosenberg R, Blomqvist M, Nilsson CH, Cederwall H, Dimming A (2004) Marine quality assessment by use of benthic species-abundance distributions: a proposed new protocol within the European Union Water Framework Directive. Mar Pollut Bull 49:728–739
Rosenberg R, Davey E, Gunnarsson J, Norling K, Frank M (2007) Application of computer-aided tomography to visualize and quantify biogenic structures in marine sediments. Mar Ecol Prog Ser 331:23–34
Solan M, Kennedy R (2002) Observation and quantification of *in situ* animal–sediment relations using time-lapse sedi-

ment profile imagery (t-SPI). Mar Ecol Prog Ser 228: 179–191

Vopel K, Thistle D, Rosenberg R (2003) Effect of the brittle star *Amphiura filiformis* (Amphiuridae, Echinodermata) on oxygen flux into the sediment. Limnol Oceanogr 48: 2034–2045

Welsh DT (2003) It's a dirty job but someone has to do it: the role of marine benthic macrofauna in organic matter turnover and nutrient recycling to the water column. Chem Ecol 19:321–342

Woodley JD (1975) The behaviour of some amphiurid brittle-stars. J Exp Mar Biol Ecol 18:29–46

Editorial responsibility: Otto Kinne, Oldendorf/Luhe, Germany

Submitted: August 27, 2007; Accepted: February 22, 2008
Proofs received from author(s): June 19, 2008